

## Bound magnetic polarons in the very dilute regime

Yu. G. Kusrayev,<sup>1</sup> K. V. Kavokin,<sup>1</sup> G. V. Astakhov,<sup>2,\*</sup> W. Ossau,<sup>2</sup> and L. W. Molenkamp<sup>2</sup>

<sup>1</sup>*A. F. Ioffe Physico-Technical Institute, Russian Academy of Sciences, 194021 St. Petersburg, Russia*

<sup>2</sup>*Physikalisches Institut (EP3), Universität Würzburg, 97074 Würzburg, Germany*

(Received 11 September 2007; published 12 February 2008)

We study bound magnetic polarons (BMPs) in a very diluted magnetic semiconductor  $\text{Cd}_{1-x}\text{Mn}_x\text{Te}$  ( $x < 0.01$ ) by means of site selective spectroscopy. In zero magnetic field we have detected a broad and asymmetric band with a characteristic spectral width of about 5 meV. When external magnetic fields are applied an additional line appears in the emission spectrum. Remarkably, the spectral width of this line is reduced greatly down to 240  $\mu\text{eV}$ . We attribute such unusual behavior to the formation of BMPs, effected by sizable fluctuations of local magnetic moments. The modifications of the optical spectra have been simulated by the Monte Carlo method and calculated within an approach considering the nearest Mn ion. A quantitative agreement with the experiment is achieved without use of fitting parameters. It is demonstrated that the low-energy part of the emission spectra originates from the energetic relaxation of a complex consisting of a hole and its nearest Mn ion. It is also shown that the contribution to the narrow line arises from the remote Mn ions.

DOI: 10.1103/PhysRevB.77.085205

PACS number(s): 75.50.Pp, 78.20.Ls, 75.30.Hx

### I. INTRODUCTION

One of the intriguing phenomena observed in diluted magnetic semiconductors (DMSs) is the formation of bound magnetic polarons.<sup>1,2</sup> The bound magnetic polaron (BMP) is a local ordering of magnetic moments induced by the exchange interaction with a localized carrier. Most BMP studies, both experimental and theoretical, have been performed so far in a regime of the mean-field approach (when  $N_{\text{Mn}}a_B^3 \gg 1$ ).<sup>3-8</sup> Here,  $N_{\text{Mn}} = xN_0$  is the concentration of magnetic ions,  $N_0$  is the concentration of cations, and  $a_B$  is the localization radius. This approach implies that the localized carrier interacts with an infinite number of  $\text{Mn}^{2+}$  ions, and hence it is typically applicable for high and moderate manganese concentrations ( $x > 0.01$ ). At present the systems with a countable number of magnetic moments attract growing interest.<sup>9</sup> This corresponds to the very dilute regime  $N_{\text{Mn}}a_B^3 \ll 1$ , i.e., when on average one carrier interacts with one (or few) Mn ion(s). Clearly, under this condition the mean-field approach is not an appropriate model.

Up to now bound magnetic polarons have not been observed in a very dilute regime. The reason for this is that their observation requires that the polaron formation time  $\tau_F$  be shorter than the lifetime  $\tau$  of nonequilibrium carriers,  $\tau_F < \tau$ . In DMSs with  $x \geq 0.1$  this condition is fulfilled. However, in samples with lower Mn concentrations,  $x \leq 0.01$ , the polaron formation time,  $\tau_F$ , is of the order of  $10^{-4} - 10^{-6}$  s.<sup>10,11</sup> Therefore, the BMP formation process is interrupted by exciton recombination (with a characteristic time  $\tau_0 \sim 10^{-9}$  s).<sup>12</sup>

In this paper we study BMPs in bulk  $\text{Cd}_{1-x}\text{Mn}_x\text{Te}$  samples with a very low Mn concentration ( $x < 0.01$ ), where the condition  $N_{\text{Mn}}a_B^3 \ll 1$  is satisfied. In order to avoid the above problem of BMP detection in the very dilute regime, we use resonant (selective) excitation of donor-acceptor (DA) pairs with transition energies<sup>4</sup>

$$E_{DA} = E_g - E_D - E_A - e^2/\epsilon\rho. \quad (1)$$

Here,  $E_D$  and  $E_A$  are binding energies of donors and acceptors, respectively,  $E_g$  is the band gap, and  $\epsilon$  is the dielectric

constant in  $\text{Cd}_{1-x}\text{Mn}_x\text{Te}$ . As follows from Eq. (1), by changing the excitation energy  $E_{ex} = E_{DA}$  one can selectively excite pairs with a given DA separation  $\rho$ . Because of the weak overlap of the donor and acceptor wave functions, the recombination time  $\tau$  of pairs with large  $\rho$  can be rather long. It can be estimated as  $\tau_0 \exp(2\rho/a_D)$ , where  $a_D \approx 60$  Å is the Bohr radius of the donor-bound electron, and  $\tau_0$  is of the order of the excitonic recombination time. For the values of  $\rho \approx 460$  Å, typical for the donor and acceptor concentrations we work with, one can evaluate  $\tau \approx 10^{-3}$  s  $> \tau_F$ . As a result the bound magnetic polaron forms before the pair has recombined. Without polaronic effects, such resonantly excited pairs should manifest themselves in emission spectra as a narrow line, whose width is determined either by the inverse recombination time ( $\hbar/\tau$ ) or by the laser linewidth.

### II. EXPERIMENT

The bulk  $\text{Cd}_{1-x}\text{Mn}_x\text{Te}$  samples with Mn concentrations  $x = 0.003, 0.005, 0.02$  have been grown by the Bridgman technique. The crystals are nominally undoped. The concentration of residual impurities (both donors and acceptors) is about  $10^{16}$  cm<sup>-3</sup>, which is much lower than the Mn concentration  $N_{\text{Mn}}$ . As-grown crystals are usually *p* type due to excess of Te or Cd vacancies. It is worth noting that, for acceptors with the Bohr radius  $a_B = 10$  Å and  $x = 0.005$  ( $N_{\text{Mn}} = 7 \times 10^{19}$  cm<sup>-3</sup>), the parameter  $N_{\text{Mn}}a_B^3$  is equal to 0.07. In the experiments, we used  $4 \times 4 \times 0.3$  mm<sup>3</sup> pieces cleaved out along the (110) plane from the massive monocrystals. All the measurements were carried out at a temperature  $T = 1.6$  K. External magnetic fields were applied either perpendicular to the sample plane (Faraday geometry), or in the sample plane (Voigt geometry). The photoluminescence (PL) was excited by a He-Ne laser or a tunable Ti:sapphire laser pumped by an Ar-ion laser. The excitation density was about 5 W/cm<sup>2</sup>. The laser beam was directed onto the samples at the angle close to the normal (axis [110]), and the emission was registered in the backscattering geometry. A polarizer (in

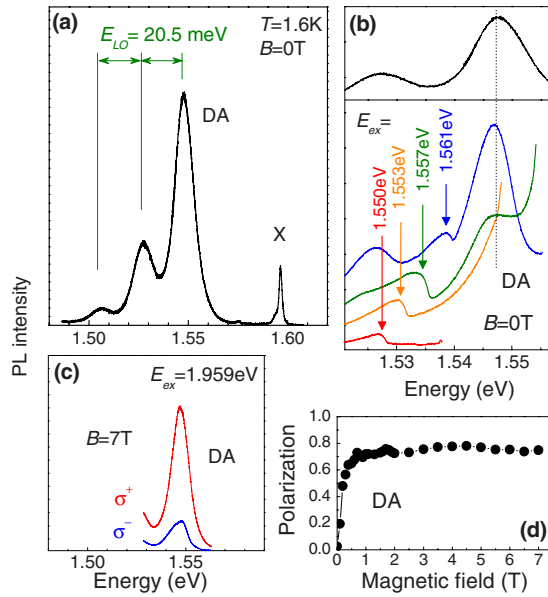


FIG. 1. (Color online) (a) Zero-field PL spectrum of the  $\text{Cd}_{0.995}\text{Mn}_{0.005}\text{Te}$  sample excited by a He-Ne laser ( $E_{ex} = 1.959$  eV). (b) PL spectra under quasiresonant excitation, the excitation energies ( $E_{ex}$ ) being shown in the panel. The arrows indicate emission bands which are related to the BMP formation. PL in the same spectral range but under nonresonant excitation [as in (a)] is given in the upper part for comparison. (c) PL spectra of DA pairs recorded in  $\sigma^+$  and  $\sigma^-$  circular polarizations in an external magnetic field  $B = 7$  T applied in Faraday geometry. The excitation conditions are the same as in (a). (c) Degree of circular polarization vs magnetic field detected at the DA band.

combination with a quarter-wave plate) was (were) used to linearly (circularly) polarize the excitation. The degree of PL polarization was detected with the use of a photoelastic modulator and of a two-channel photon counter.

We found a qualitatively very similar behavior in all the samples studied. In the following, we present experimental results for one piece cleaved out from the bulk  $\text{Cd}_{0.995}\text{Mn}_{0.005}\text{Te}$  sample. Figure 1(a) shows the PL spectrum excited above the CdTe band gap  $E_g$  (He-Ne laser with  $E_{ex} = 1.959$  eV). The high-energy line (X) is attributed to the bound exciton. In the low-energy part of the PL spectrum, we observe a broad band associated with recombination of DA pairs, as well as its phonon replicas. These replicas are separated by 20.5 meV, which corresponds to the LO-phonon energy in CdTe.<sup>13</sup> Application of external magnetic fields in Faraday geometry results in the circularly polarized emission already in low fields [Fig. 1(c)]. Such a behavior is typical for magnetic semiconductors. Figure 1(d) demonstrates the degree of circular polarization vs magnetic field detected at the DA band. It saturates rapidly at the 75% level.

In order to study bound magnetic polarons, we use the site selective spectroscopy.<sup>14</sup> We resonantly excite DA pairs and record BMP spectra shifted toward lower energies with respect to the excitation energy  $E_{ex}$  (the Stokes shift). A set of PL spectra for different  $E_{ex}$  is presented in Fig. 1(b). An emission band (indicated by arrows), superimposed on the DA photoluminescence, clearly follows the laser line. This

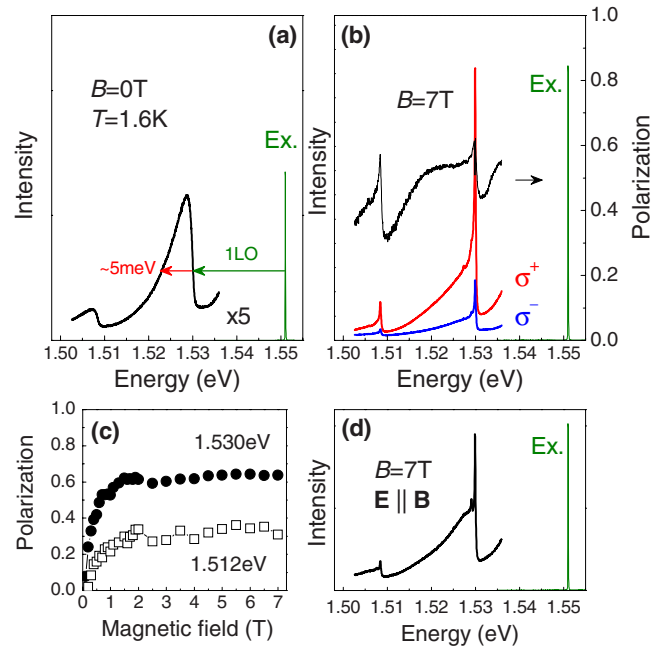


FIG. 2. (Color online) (a) BMP spectrum obtained under resonant excitation (Ex.) to the DA band ( $E_{ex} = 1.551$  eV) in zero magnetic field. (b) BMP and BMP-polarization spectra obtained under the same excitation conditions as in (a) but in magnetic field  $B = 7$  T applied in Faraday geometry. (c) Degree of circular polarization vs magnetic field detected at different energies. (d) BMP spectrum obtained in magnetic field  $B = 7$  T applied in Voigt geometry when the polarization axis of the excitation ( $E$ ) is parallel to the field direction ( $E \parallel B$ ).

behavior is a fingerprint of the BMP formation. The most pronounced results have been obtained for  $E_{ex} = 1.551$  eV, as shown also in Fig. 2. In order to avoid scattered light from the laser, we detect such BMP spectra at the first phonon replica.

In zero magnetic field, the BMP spectrum shows up as an asymmetric band with a 5 meV tail toward low energies [Fig. 2(a)]. Our estimations (given below) show that this value is in agreement with the calculated values of the BMP energy and its root-mean-square fluctuations. Such a behavior is a distinct deviation from the case of high Mn concentrations ( $N_{\text{Mn}}a_B^3 \gg 1$ ), where the Stokes shift is larger than the linewidth and gives rise to a separate emission line shifted from the excitation by the BMP energy.<sup>14</sup>

The most drastic changes, however, occur in external magnetic fields applied in Faraday geometry [Fig. 3(a)]. A line appears at the resonant energy (i.e., there is no Stokes shift at all).<sup>15</sup> With growing magnetic field, the amplitude of this line increases and the width reduces greatly. In strong enough magnetic fields ( $B > 3$  T), the full width at half maximum (FWHM) saturates on a 240  $\mu\text{eV}$  level [see also Fig. 2(b)]. The circular polarization of this line is about 65%, and its dependence on the magnetic field [Fig. 2(c)] follows that for the DA emission under nonresonant excitation [Fig. 1(d)]. One more feature of this line: its intensity reduces if the excitation light is linearly polarized along the magnetic field direction in Voigt geometry [see Fig. 2(d)]. However, a

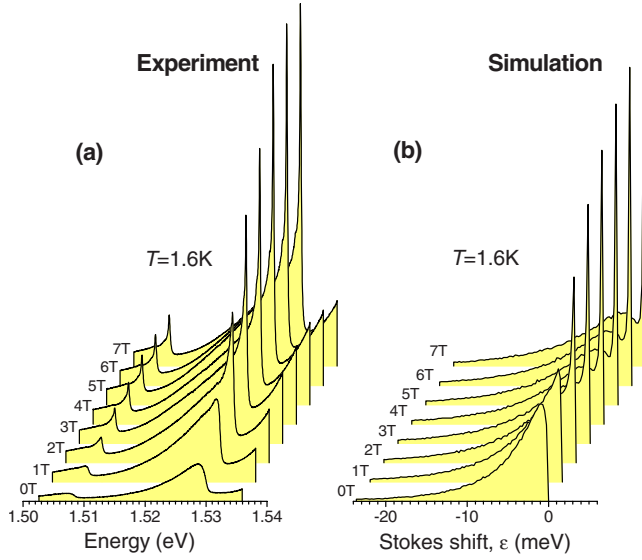


FIG. 3. (Color online) Evolution of BMP spectra with growing magnetic field: (a) experiment and (b) the Monte Carlo simulation. Note that in (b) no fitting parameters are used. The PL spectra are shifted for clarity.

deviation of the field direction from the sample plane, or of the polarization axis from the field direction, restores the amplitude of this line.

As we show in Sec. (3), the evolution of PL spectra presented in Fig. 3(a) cannot be described in terms of the mean-field theory, and therefore an alternative approach is required. First, we discuss the asymmetric band observed in zero magnetic field. Resonant excitation generates DA pairs with a certain energy  $E_{DA}=E_{ex}$  depending on the donor-acceptor distance  $\rho$  [pairs (i) and (iii) in Fig. 4(a)]. DA pairs

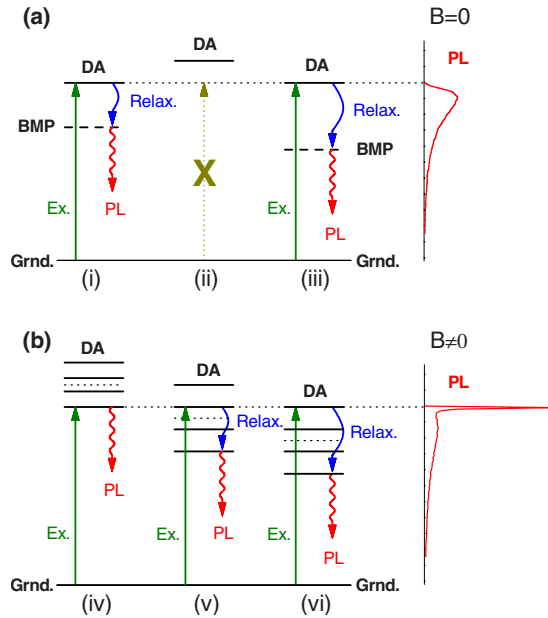


FIG. 4. (Color online) Formation of BMP spectra under selective excitation (Ex.) in (a) zero and (b) strong magnetic fields. The roman numerals in parentheses enumerate different DA pairs.

with transition energies, different from the excitation energy  $E_{DA} \neq E_{exc}$ , are not excited [pair (ii) in Fig. 4(a)]. We attribute the observation of the asymmetric band in Fig. 2(a) to the BMP formation accompanied by the relaxation to the ground state. The dominant contribution to the polaron shift comes from the hole. This is because the absolute value of the  $p$ - $d$  exchange constant is larger than the absolute value of the  $s$ - $d$  exchange, and the Bohr radius of the acceptor is smaller than that of the donor.<sup>1,2</sup> The linewidth is then explained by the dispersion of the polaron shifts induced by static fluctuations of Mn concentration. For instance, the pair (iii) in Fig. 4(a) shows a larger polaron shift than the pair (i). Because less than one Mn, on average, falls into the volume within the acceptor Bohr radius, the root-mean-square fluctuations appear to be comparable with the polaron shift. Its value can be estimated from the linewidth in Fig. 2(a),  $\Gamma \approx 5$  meV.

Strong enough magnetic fields suppress the polaron formation,<sup>16</sup> and one would expect the low-energy tail to disappear. However, our experiments show the opposite behavior: The tail preserves, while a narrow, intense line appears. We suggest the following explanation. Acceptor (donor) states are split in the exchange field of Mn ions polarized by the external magnetic field. The photon absorption by a certain DA pair leads to the population of one of the Zeeman sublevels [Fig. 4(b)]. Relaxation from the higher-lying sublevels to the lowest sublevel [pairs (v) and (vi) in Fig. 4(b)] results in the low-energy tail. The characteristic width of this tail does not change with magnetic fields because the Zeeman splittings disperse in the same manner as the polaron shifts, i.e., due to static fluctuations of the Mn concentration. If the lowest Zeeman sublevel of the DA pair is excited [pair (iv) in Fig. 4(b)], further relaxation is not possible, and the narrow line is observed at the excitation energy. With growing magnetic fields, the width of this line should decrease and stabilize in the fields saturating the magnetization of magnetic ions ( $B > 3$  T).

It is now clear why the narrow peak is suppressed, when the polarization axis of the excitation light is exactly parallel to the magnetic field direction: Due to the optical selection rules, the excitation to the ground state [pair (iv) in Fig. 4(b)] is forbidden in this configuration. However, even a small deviation from this geometry gives rise to the perpendicular-to-field component of the polarization vector, and the peak is restored.

### III. THEORY

In order to calculate the PL spectra under selective excitation, one needs to find the distribution function of the Stokes shift induced by the polaron formation in zero magnetic field. On the other hand, in strong magnetic fields the distribution function is determined by the Zeeman splitting dispersion. The hole (electron) spins interact with Mn ions via the  $p$ - $d$  ( $s$ - $d$ ) exchange interaction. In the case of localized carriers this interaction can be written as

$$\hat{H}_{sd} = \alpha \sum_i \vec{s}_e \cdot \vec{S}_i \Psi_e^2(\vec{r}_i), \quad (2)$$

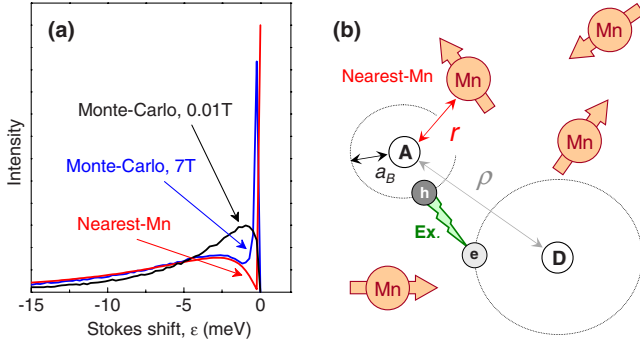


FIG. 5. (Color online) (a) Calculations of the PL spectra by the Monte Carlo method and within the approach considering the nearest-Mn ion. Note that the nearest-Mn approach gives the same result for zero and strong magnetic fields. (b) Random distribution of acceptors (A), donors (D), and Mn ions.

$$\hat{\mathcal{H}}_{pd} = \frac{\beta}{3} \sum_i \vec{J} \cdot \vec{S}_i \Psi_h^2(\vec{r}_i), \quad (3)$$

where  $\vec{s}_e$  and  $\vec{J}$  are the electron and hole spin operators, and  $\Psi_e$  and  $\Psi_h$  are their wave functions, respectively.  $\vec{S}_i$  is the spin operator of the  $i$ th Mn ion, and  $\vec{r}_i$  is the position vector of the Mn ion. The exchange constants in  $\text{Cd}_{1-x}\text{Mn}_x\text{Te}$  are  $\alpha = 14\,850 \text{ meV } \text{\AA}^3$  and  $\beta = 59\,400 \text{ meV } \text{\AA}^3$ . The donor and acceptor Bohr radii are approximately equal to 60 and  $10 \text{ \AA}$ , respectively. This implies that the spin splitting of the Mn ion, separated from the acceptor (donor) by the Bohr radius, is 1.28 meV ( $1.5 \mu\text{eV}$ ). In other words, at the temperature  $T = 1.6 \text{ K}$  ( $k_B T = 0.14 \text{ meV}$ ) the electron contribution can be neglected, and all the Mn spins in the vicinity of the acceptor are aligned along the exchange field of the hole. The hole exchange energy in the ground state is  $E_h = \frac{5}{4} \beta \sum_i \Psi_h^2(\vec{r}_i)$ . Its mean value averaged over all Mn configurations is  $\langle E_h \rangle = \frac{5}{4} \beta N_0 x$ , where  $N_0 = 0.015 \text{ \AA}^{-3}$  is the concentration of cations. For  $x = 0.005$ ,  $\langle E_h \rangle = 5.0 \text{ meV}$ . The root-mean-square fluctuation of the hole exchange energy  $\delta E_h = \sqrt{\langle E_h^2 \rangle - \langle E_h \rangle^2} = \frac{5}{4} \beta \sqrt{N_0 x} \int \Psi_h^4 d^3 r - (N_0 x)^2$  is equal to 5.9 meV. It follows from these estimations that the fluctuations of the exchange energy and its mean value are nearly the same. Therefore, the Gaussian statistics and, as a consequence, the mean-field approach are not applicable.

In case of low Mn concentrations, it is difficult to obtain an analytical solution for the Stokes-shift distribution function. We calculated the PL spectra under selective excitation numerically, with the Monte Carlo method. The following procedure was used. First, a random distribution of magnetic ions inside a sphere with the radius equal to ten acceptor Bohr radii,  $10a_B$ , is generated [see also Fig. 5(b)].<sup>17</sup> Each Mn ion is assigned a random spin orientation in accordance with the equilibrium distribution for the given temperature and magnetic field strength. Then, the total exchange field acting on the hole bound to the acceptor placed in the center of the sphere is calculated. After that, the eigenstates of the hole in this total exchange field and the transition probabilities to

these states are evaluated. For each spatial distribution of Mn ions, polaron energies are determined. This is done by adding the exchange field of the hole, acting on Mn ions, to the external magnetic field, and generating the distribution of Mn spin configurations in this total field. The polaron energy is then found as the ground-state energy of the hole in the exchange field produced by the Mn spins. The Stokes shift is calculated as the energy difference between the initial (without polaron) and the final (polaron) states. Finally, the distribution function of the Stokes shift is obtained after summation over 50 000 realizations.

The calculated PL spectra for different magnetic fields are shown in Fig. 3(b). Not only qualitative, but also quantitative agreement with experimental data [compare with Fig. 3(a)] is achieved. Note that no fitting parameters are used in the calculation.

Because of low Mn-ion numbers in the vicinity of the acceptor (on average there are 0.3 Mn ions inside the sphere of radius  $a_B$ ) it is natural to assume that the nearest Mn ions give dominant contributions to the Stokes shifts [Fig. 5(b)]. We now consider this approach in detail. In an external magnetic field, the hole states are split into four sublevels characterized by the different projection  $J_z$  of the hole angular momentum on the field direction. One of them, with  $J_z = 3/2$ , is a ground state. The contribution of this state to the PL spectrum is a delta function  $\delta(\epsilon)$  (if neglecting the homogeneous broadening) as shown in Fig. 4(b) [pair (iv)]. Excitation into one of the three other states is followed by relaxation to the ground state [pairs (v) and (vi) in Fig. 4(b)]. The shift of the emission energy with respect to the excitation energy is therefore described by the distribution function of the nearest (to the hole) Mn ion over the energy of its exchange interaction with the hole,  $F_{NN}(\epsilon)$ . Under unpolarized excitation, the distribution function  $F(\epsilon)$  of the Stokes shift  $\epsilon$  is written as

$$F(\epsilon) = W_{3/2} \delta(\epsilon) + W_{1/2} F_{NN}(3\epsilon/2\epsilon_0) + W_{1/2} F_{NN}(3\epsilon/4\epsilon_0) + W_{3/2} F_{NN}(\epsilon/2\epsilon_0), \quad (4)$$

where  $W_{3/2} = 3/4$  and  $W_{1/2} = 1/4$  are the probabilities to excite the hole with  $J_z = \pm 3/2$  and  $J_z = \pm 1/2$ , respectively. The characteristic exchange energy is  $\epsilon_0 = \frac{5}{4} \beta \Psi_h^2(0) = 23.6 \text{ meV}$ . The probability  $dP_{NN}(r)$  that the nearest Mn ion is located in the spherical layer  $(r, r+dr)$  [see Fig. 5(b)] is given by the probability to find one Mn ion in this spherical layer ( $xN_0 4\pi r^2 dr$ ), and the probability  $P_0(r)$  that there are no Mn ions inside the sphere of radius  $r$ . Here,  $P_0(r)$  is obtained from the Poisson distribution  $P_n(\bar{n}) = \frac{\bar{n}^n}{n!} \exp(-\bar{n})$  by putting  $n=0$  and  $\bar{n} = \frac{4}{3} \pi r^3 x N_0$ . Then one writes

$$dP_{NN}(r) = 4\pi r^2 x N_0 \exp(-4\pi r^3 x N_0/3) dr. \quad (5)$$

Recall that the energy of the exchange interaction between the hole and Mn ion depends on the distance  $r$  as  $\Psi_h^2(r)$ , i.e.,  $\epsilon(r) = \epsilon_0 \exp(-2r/a_B)$  and  $dr = -a_B/(2\epsilon) d\epsilon$ . Finally, one obtains the distribution function over energy  $\epsilon$  as  $F_{NN} = dP_{NN}/d\epsilon$

$$F_{NN}(\varepsilon/\varepsilon_0) = \frac{3\gamma}{\varepsilon} \left( \ln \frac{\varepsilon}{\varepsilon_0} \right)^2 \exp \left[ \gamma \left( \ln \frac{\varepsilon}{\varepsilon_0} \right)^3 \right], \quad (6)$$

with  $\gamma = (\pi/6) x N_0 a_B^3$ .

Figure 5(a) shows that the PL spectra in high magnetic fields are well described within the nearest-Mn approach. However, the agreement becomes worse for small  $\varepsilon$  in zero magnetic field, while the high-energy tail is still described quite well. The reason is that the relaxation of the complex “hole+nearest-Mn ion” is not possible under excitation to the ground state, and the Stokes shift is absent. This results in a  $\delta$ -function peak appearing in zero as well as in high magnetic fields [first term in Eq. (4)]. In reality, the contribution to the Stokes shift for  $\varepsilon \ll \varepsilon_0$  arises from several distant ( $r \gg a_B$ ) Mn ions. In weak magnetic fields, the spins of these distant ions are disordered, and their orientation induced by the exchange field of the hole results in the energy lowering. In strong magnetic fields, the spins are already oriented at the moment of excitation, further relaxation does not occur, which manifests itself as the appearance of the narrow peak at  $\varepsilon=0$ .

#### IV. CONCLUSIONS

With the use of the site selective spectroscopy of residual DA pairs in bulk  $\text{Cd}_{1-x}\text{Mn}_x\text{Te}$  samples, we are able to observe the formation of bound magnetic polarons in a very dilute ( $x < 0.01$ ) regime. Under selective excitation, the PL spectra show an asymmetric band with the low-energy tail and an additional very narrow peak springing up in external magnetic fields. This behavior cannot be described in terms of the mean-field approach, frequently applied to diluted magnetic semiconductors. Our findings suggest that the low-energy tail is formed due to the exchange interaction of the hole (bound to the acceptor) with the nearest-Mn ion. Unexpectedly, the dominant contribution to the width of the narrow peak arises from the interaction with several more distant Mn ions.

#### ACKNOWLEDGMENTS

This research was supported by the DFG (436 RUS 113/843 and SPP 1285) as well as the RFBR. We thank R. R. Galazka (Institute of Physics, Warsaw, Poland) for providing us with high quality samples.

\*Also at A. F. Ioffe Physico-Technical Institute, RAS, 194021 St. Petersburg, Russia; astakhov@physik.uni-wuerzburg.de

<sup>1</sup>J. K. Furdyna, *J. Appl. Phys.* **64**, R29 (1988).

<sup>2</sup>P. A. Wolff, in *Semiconductors and Semimetals*, edited by J. K. Furdyna and J. Kossut (Academic, London, 1988), Vol. 25.

<sup>3</sup>D. Heiman, J. Warnock, P. A. Wolff, R. Kershaw, R. Ridgely, K. Dwight, and A. Wold, *Solid State Commun.* **52**, 909 (1984).

<sup>4</sup>T. H. Nhung, R. Planel, C. Benoit a la Guillaume, and A. K. Bhattacharjee, *Phys. Rev. B* **31**, 2388 (1985).

<sup>5</sup>M. Nawrocki, R. Planel, G. Fishman, and R. Galazka, *Phys. Rev. Lett.* **46**, 735 (1981).

<sup>6</sup>M. Bugajski, P. Becla, P. A. Wolff, D. Heiman, and L. R. Ram-Mohan, *Phys. Rev. B* **38**, 10512 (1988).

<sup>7</sup>T. Dietl and J. Spalek, *Phys. Rev. Lett.* **48**, 355 (1982); *Phys. Rev. B* **28**, 1548 (1983).

<sup>8</sup>L. R. Ram-Mohan and P. A. Wolff, *Phys. Rev. B* **38**, 1330 (1988).

<sup>9</sup>L. Besombes, Y. Léger, L. Maingault, D. Ferrand, H. Mariette, and J. Cibert, *Phys. Rev. Lett.* **93**, 207403 (2004).

<sup>10</sup>D. Scalbert, J. Cernogora, and C. Benoit A La Guillaume, *Solid*

*State Commun.* **66**, 571 (1988).

<sup>11</sup>T. Strutz, A. M. Witowski, and P. Wyder, *Phys. Rev. Lett.* **68**, 3912 (1992).

<sup>12</sup>G. Mackh, W. Ossau, D. R. Yakovlev, A. Waag, G. Landwehr, R. Hellmann, and E. O. Göbel, *Phys. Rev. B* **49**, 10248 (1994).

<sup>13</sup>D. J. Olego, P. M. Raccach, and J. P. Faurie, *Phys. Rev. B* **33**, 3819 (1986).

<sup>14</sup>J. Warnock, R. N. Kershaw, D. Ridgely, K. Dwight, A. Wold, and R. R. Galazka, *J. Lumin.* **34**, 25 (1985); T. Itoh and E. Komatsu, *ibid.* **38**, 266 (1987); B. P. Zakharchenya and Yu. G. Kusrayev, *JETP Lett.* **50**, 199 (1989).

<sup>15</sup>In continuous wave (cw) experiments it is not possible to separate the emission from the laser light at the energy of excitation. However, this can be easily done at the phonon replicas of PL lines, where the contribution of scattered light is negligible.

<sup>16</sup>V. F. Aguekian, L. K. Gridneva, and A. Yu. Serov, *Solid State Commun.* **85**, 859 (1993).

<sup>17</sup>Note in Ref. 4, in order to calculate BMP energies, the magnetic ions in a sphere of radius  $R \sim 1.5a_B$  were considered.